J Braz. Soc. Mech. Sci. Eng.
DOI 10.1007/s40430-014-0147-x

TECHNICAL PAPER

Nb–Cr complex carbide coatings on AISI D2 steel produced by the TRD process

Fabio Enrique Castillejo · Jhon Jairo Olaya · José Manuel Arroyo-Osorio

Received: 8 September 2012 / Accepted: 15 April 2013

Abstract Nb–Cr complex carbide coatings were produced onto AISI D2 steel by the thermo-reactive diffusion process to improve the surface hardness and corrosion resistance of this tool steel. The carbide coating treatment was performed using molten borax added with ferroniobium, ferrochrome and aluminum at temperatures of 1,223, 1,293 and 1,363 K during 2, 3, 4 and 5 h. The coating layers were characterized by optical and Scanning Electron Microscopy, X-ray diffraction, energy-dispersive X-ray spectroscopy and X-ray fluorescence spectrometry. The coating growth rates were evaluated, and a model of the layer thickness as a function of the treatment time and temperature was established. The hardness of the coating was measured by nanoindentation, and its resistance to corrosion was evaluated with electrochemical tests of potentiodynamic polarization. The produced carbide layers presented a homogeneous thickness as well as an improved hardness and corrosion resistance as compared to the uncoated steel.

Keywords Thermo-reactive diffusion coatings · Nb–Cr complex carbides · Corrosion · Hardness

Technical Editor: Alexandre Abrão.

F. E. Castillejo (✉)
Departamento de Ciencias Básicas, Universidad Santo Tomás, Bogotá DC, Colombia
e-mail: fabiocastillejo@usantotomas.edu.co

J. J. Olaya · J. M. Arroyo-Osorio
Departamento de Ingeniería Mecánica, Universidad Nacional de Colombia, Bogotá DC, Colombia
e-mail: jjolayaf@unal.edu.co

J. M. Arroyo-Osorio
e-mail: jmarroyoo@unal.edu.co

List of symbols

x	Carbide layer thickness, cm
D	Diffusion coefficient, cm^2/s
t	Processing time, s
R	Gas constant, J/(mol K)
Q	Activation energy, kJ/mol
T	Absolute temperature, K

1 Introduction

The durability of a part subjected to different environmental conditions and stresses depends strongly on its surface properties. Treatments that modify surfaces through the deposition of transition metal carbide or nitride layers have improved the tribological performance of tools and machine elements subjected to severe wear conditions. These coatings are commonly produced on an industrial scale using physical vapor deposition (PVD) or chemical vapor deposition (CVD) [9]. These techniques are limited because their implementation requires the use of complex and costly equipment that must be operated at high-vacuum conditions.

For substrates containing more than 0.3 wt% C, the application of hard coatings by the thermo-reactive diffusion process (TRD) is a more economical alternative. The coatings that can be achieved through this process have good adhesion to the substrate, generally low friction coefficient and homogeneous thickness [3]. In the TRD process, the work materials are immersed in a bath that contains molten borax, aluminum as a reducing agent and carbide-forming elements (CFEs) such as vanadium, chromium, titanium and niobium [2]. To produce the carbide layer, the carbide formation energy must be lower than the boron oxide (B_2O_3)

Published online: 26 March 2014

Table 1 Chemical composition of the AISI D2 steel substrates

% C	% Cr	% Mn	% Si	% W	% Fe
1.5	11.5–12.5	0.15–0.45	0.1–0.4	0.6–0.9	Balance

formation energy [1]. This condition is not met in the particular case of titanium, given that the formation energy of the titanium carbide is higher; thus, the boron atoms do not oxidize but instead remain free to diffuse toward the steel matrix where they combine with the iron to form layers of Fe_2B or FeB [8].

Several authors have reported on the synthesis of binary metal carbide coatings by the TRD process and have characterized the microstructure, hardness and wear resistance of the fabricated coatings. Oliveira et al. worked on the production of VC and NbC coatings onto substrates of AISI H13, AISI D2 and AISI M2 steels and reported a coating hardness of up to 2,300 HV [4]. In other works, the growth kinetics of NbC coating onto AISI 1040 steel substrate [7] and of FeB coating onto AISI 4140 steel substrates [5] have been studied, and it was found that the thickness of the coating layer obtained for binary systems such as NbC and VC is a function both of the temperature of the process and of the treatment time, having a growth rate in agreement with the Arrhenius equation. In all of these investigations, only one CFE was added to the borax bath to form only a single type of carbide coating. In this work, we produced coatings by TRD on AISI D2 steel substrates using a borax bath with two types of CFEs, Nb and Cr. Microstructure, hardness and electrochemical analyses were performed and the growth kinetics of the coatings was studied.

2 Experimental procedure

The substrates were disks of AISI D2 steel, with 15-mm diameter and 4-mm thickness, whose surfaces were polished up with 1,200-grit sandpaper. All surfaces were subsequently cleaned with acetone and then immersed in isopropyl alcohol ultrasonic bath. The chemical composition of the steel, as stated by the manufacturer, is given in Table 1.

Ferroniobium Fe–Nb (64 wt% Nb) and ferrochromium Fe–Cr (69 wt% Cr) were used in a bath with the following composition: 81 wt% $Na_2B_4O_7$, 8 wt.% Fe–Nb, 8 wt% Fe–Cr and 3 wt% Al. The processing times were 2, 3, 4 and 5 h with temperatures of 1,223, 1,293 and 1,363 K. To identify the phases in the coatings as well as their preferred orientations, an X-PertPro Panalitycal diffractometer was utilized with the following settings: $\theta-2\theta$ varying from 10° to 120°, using monochromatic Cu Kα radiation with a wavelength of 1.5409 Å, working with 45 kV, 40 mA and a step size of 0.02°.

The metallographic sample surfaces were prepared by etching with 3 % Vilella's reagent and the thickness of each coating was determined using the image-analysis system of a Leco optical microscope. Ten measurements were performed on each sample to obtain the average thickness value. The hardness of each coating was determined in accordance with ISO standard 14577 using an NTH2 nanoindentor from CSM instruments outfitted with a Berkovich indenter tip. A linear load was used with an approximation speed of 2,000 nm/min, loading rate of 60 mN/min, maximum load of 30 mN and a loading dwell time of 15 s.

To determine the chemical composition a Philips MagixPro PW2440 X-ray fluorescence (XRF) spectrometer equipped with a rhodium tube operated at a maximum power of 4 kW was used. In addition, X-ray spectroscopy (EDS) at a voltage of 20 kV and collecting time of 120 s in a FEI Quanta 200 scanning electron microscope (SEM) was also performed to complement the chemical analysis.

Finally, the corrosion resistance was evaluated by the Tafel polarization measurements test following the ASTM G5 (year 1999) standard. A saturated calomel electrode and high-purity platinum were used as a reference and counter electrodes, respectively, with an exposed area of 0.196 cm^2. After 1 h of immersion in a 0.3 % NaCl electrolyte, scans were conducted in a −0.5 to 0.6 range, having a rate of 0.5 mV/s. The corrosion potential and the velocity of corrosion were obtained by Tafel extrapolation using a Gamry reference 600 potentiostat–galvanostat. A total of five corrosion tests were conducted on the substrate steel and five tests on the coated steel.

3 Results and discussion

3.1 Growth kinetics

Figure 1 shows SEM micrographs of the coatings produced at 1,363 K with treatment times of 2 and 5 h, respectively. Layers with homogeneous thickness can be observed as well as an increase in thickness as a function of the processing time, as in a typical diffusion process such as nitridation or carburization.

Figure 2 shows a plot of the coating thickness as a function of temperature and treatment time, thickness values of 4.71 ± 0.23 to 15.30 ± 0.36 μm were obtained. It can be observed that the thickness of the layers increased exponentially with treatment time and that at a given treatment time, greater thicknesses were achieved for higher treatment temperature. The process time and the treatment temperature are the most important factors

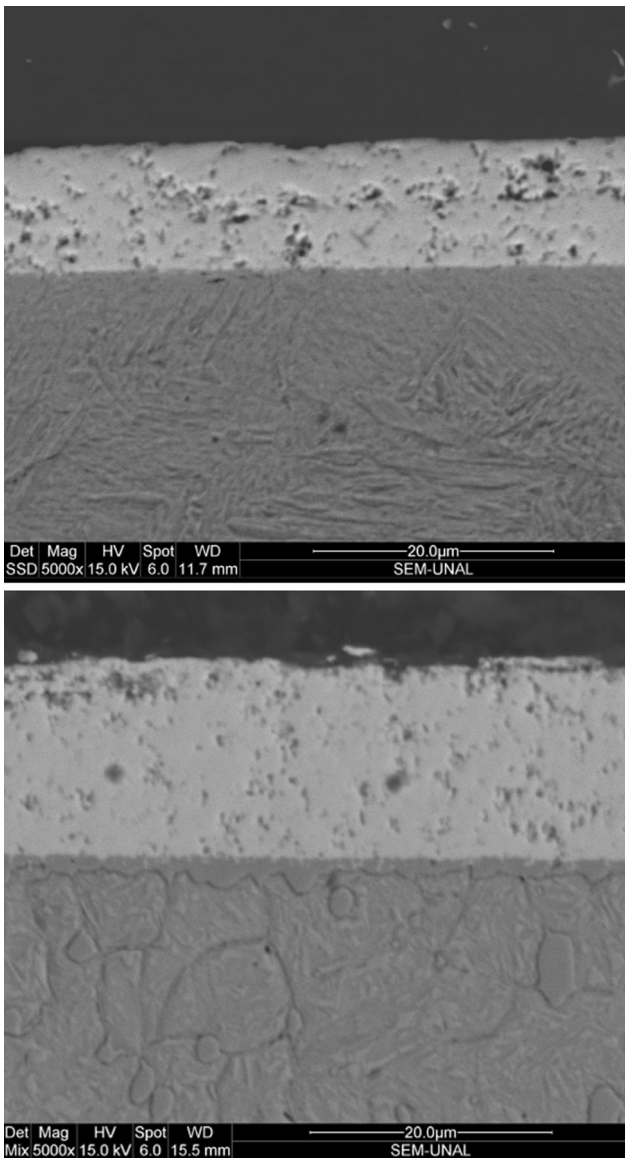

Fig. 1 SEM micrographs of the coatings synthesized at 1,363 K with treatment time of 2 h (*up*) and 5 h (*down*)

affecting the coating layer thickness because the temperature enhances diffusion of niobium, chromium and of the carbon into the carbide layer.

Given that the coating thickness clearly depends on the treatment time, the following phenomena can be assumed: (a) the growth rate of the carbide layer is controlled by the diffusion rates of the niobium and chromium atoms in the process of synthesizing carbides (b) carbon atoms from the steel substrate migrate to the surface by thermal diffusion, and (c) the growth of the coating layer is perpendicular to the surface of the treated steel [7]. The carbide layer thickness variation with time (see Fig. 2) has a parabolic evolution given by Eq. (1), where x is the carbide layer

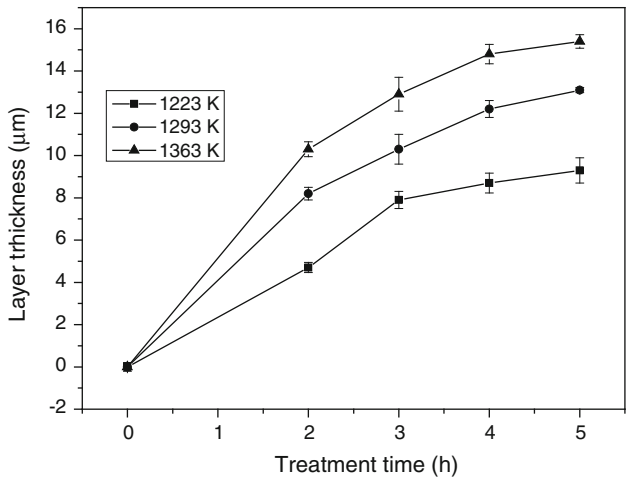

Fig. 2 Coating thickness as a function of temperature and treatment time

thickness (cm), D represents the diffusion coefficient (cm^2/s) and t is the processing time (s).

$$x^2 = D\,t \tag{1}$$

The plot of the square of the carbide layer thickness (x^2) as a function of treatment time (t) is shown in Fig. 3. Also are shown the lines obtained by a linear regression between x^2 and t experimental data. In agreement with Eq. (1), the slopes of these lines, whose values are shown in the figure, represent the diffusion coefficient (D) for each treatment temperature.

The relationship between the diffusion coefficient (D), the activation energy (Q) and the absolute process temperature (T) can be written as proposed by Arrhenius in Eq. (2), where D_0 is the frequency factor (pre-exponential constant), the Eq. (3) results from applying natural logarithm to Eq. (2).

$$D = D_0 \mathrm{e}^{-Q/(RT)} \tag{2}$$

$$\ln D = -Q/(RT) + \ln D_0 \tag{3}$$

Figure 4 shows a plot of the natural logarithm of the diffusion coefficient (D) versus the inverse of temperature (T). According to Eq. (3), the slope of the resulting straight line represents the value of the quotient of the activation energy (Q) over the gas constant (R), which yields $-Q/R = -11{,}687$, then taking $R = 8.314$ J/mol K, results that $Q = 97.165$ kJ/mol. The value of $\ln D_0$ can be determined by the intersection of the line with the vertical axis, such that $D_0 = 7.612 \times 10^{-7}$ cm^2/s.

Combining Eqs. (1) and (2) yields Eq. (4) to calculate the thickness of the coating x (µm) as a function of the absolute temperature T (K) and of the processing time t (s).

$$x = 523.48\left(t\ \mathrm{e}^{-11686.9/T}\right)^{0.5} \tag{4}$$

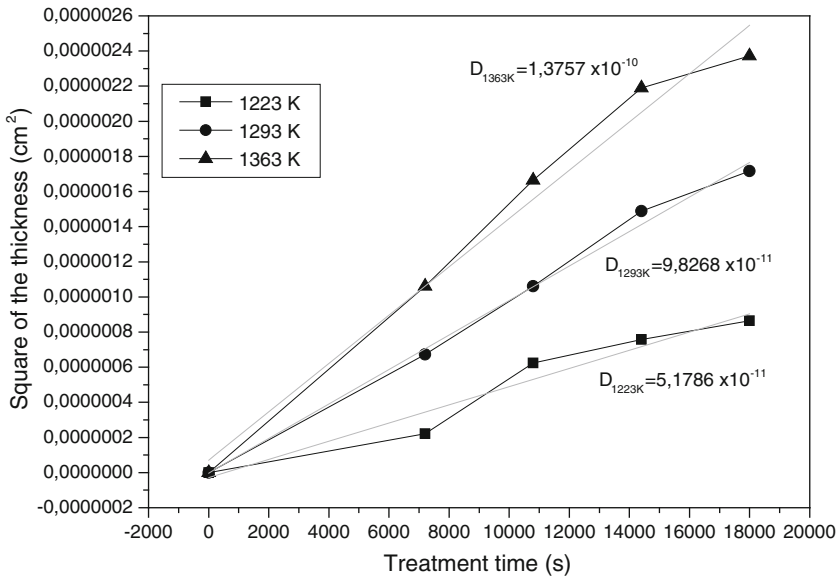

Fig. 3 Square of the layer thickness (x^2) as a function of treatment time (t) for each temperature (T) and calculated diffusion coefficient (D)

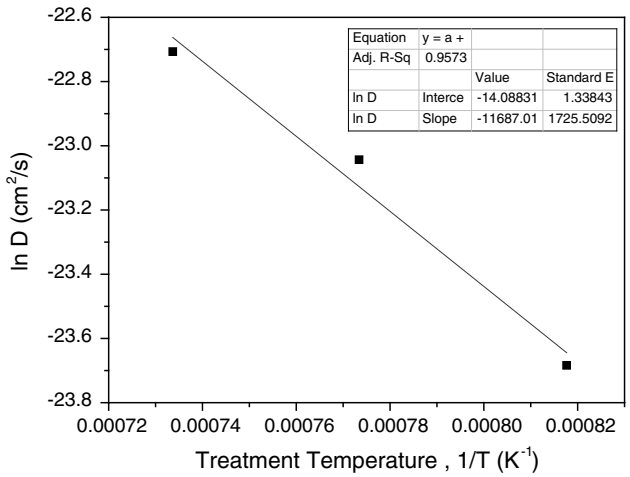

Fig. 4 Natural logarithm of D as a function of the inverse of the temperature T

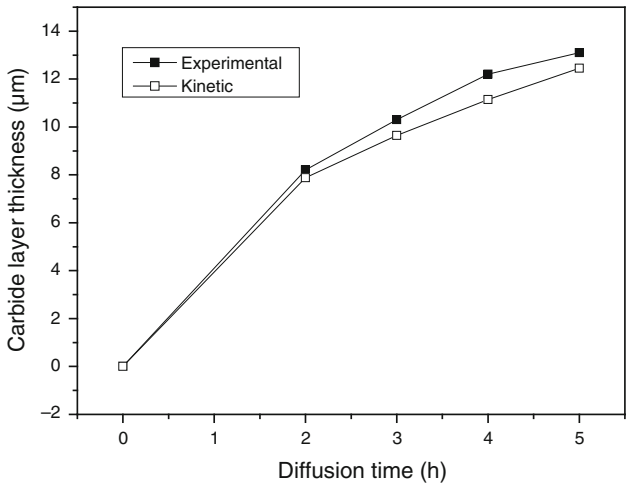

Fig. 5 Experimental and calculated data for the coating layer thickness of niobium–chromium carbide-coated AISI D2 steel at 1,293 K

Figure 5 is a comparison of the results using the Eq. (4) and the experimental data in the case of coating onto AISI D2 steel at 1,293 K. It can be observed that the Eq. (4) derived from classical kinetics closely represents the evolution of carbide layer thickness, so it can be used to predict the layer coating thickness in the TRD process.

3.2 Structural and hardness characterization

The EDS analysis (Fig. 6) of the coating showed the presence of Nb and Cr, with Nb in a greater amount. This fact is possibly due to the lower formation energy of Nb carbides (-31.8 ± 0.9 kcal) compared to the formation energy of Cr carbides (-18.0 kcal) [10]. The EDS spectrum also showed a lower iron concentration in the coating than in the bulk of the substrate.

Figure 7 shows the XRD pattern of the coating produced at 1,363 K during 4 h. The presence of NbC is observed with high-intensity peaks from the (200) and (311) planes and with low-intensity peaks from the (111), (220), (400), (420) and (422) planes of the face-centered cubic (FCC) phase. Small quantities of chromium carbide ($Cr_{23}C_6$) seem to be present on (931) and (511) planes where low-intensity peaks can be observed. Figure 8 shows a detailed view of the 2θ diffraction pattern between 86° and 88°, where the broad peak that can be seen was separated in two peaks by the deconvolution shown with one peak for niobium carbide and the other for chromium carbide. This broad peak could be due to atomic substitutions of chromium in the crystal structure of the niobium carbide. The presence of Cr in the coating was also corroborated by XRF.

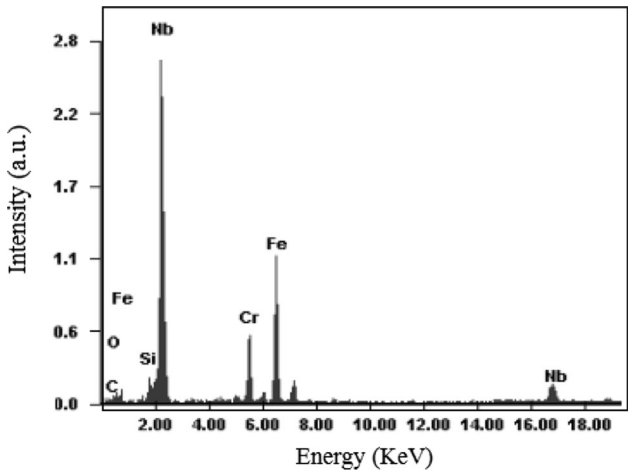

Fig. 6 EDS spectrum of the coating produced at 1,363 K during 4 h

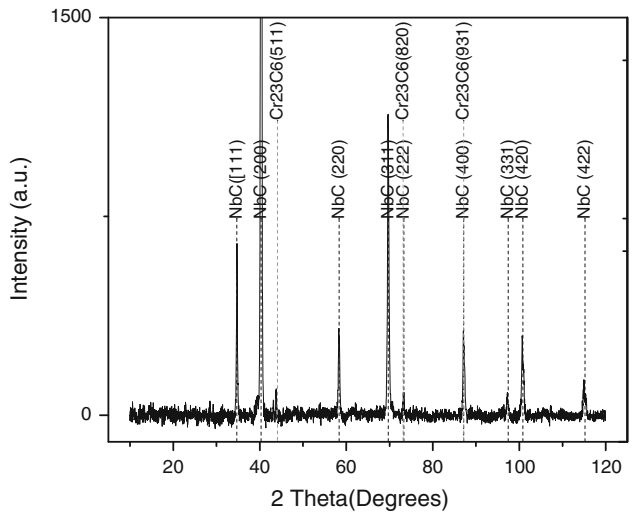

Fig. 7 X-ray diffractogram of the coating produced at 1,363 K during 4 h

The nanoindentation tests determined that the produced coating has a hardness of 27.62 ± 2.56 GPa. This hardness is greater than the hardness values previously reported for niobium carbide (23.72 ± 0.93 GPa) [4] or for chromium carbide (18.50 ± 0.35 GPa) [6]. This increase in hardness could be the result of possible atomic interchanges in the crystal structure between the two present carbides.

3.3 Electrochemical characterization

Figure 9 shows the resultant curves of the potentiodynamic test performed on the uncoated AISI D2 steel and on this steel coated with the Nb–Cr complex carbide coating deposited over the course of 4 h at a temperature of 1,363 K.

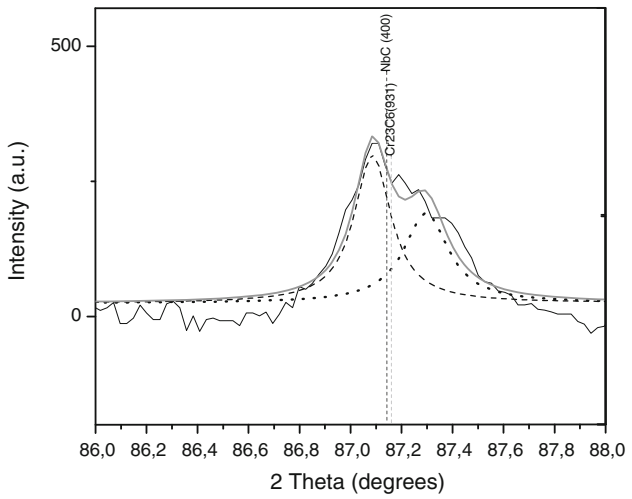

Fig. 8 Detailed view of 2θ between 86° and 88° for the X-ray diffractogram of the coating produced at 1,363 K during 4 h. The *gray curve* is a deconvolution of the broad peak

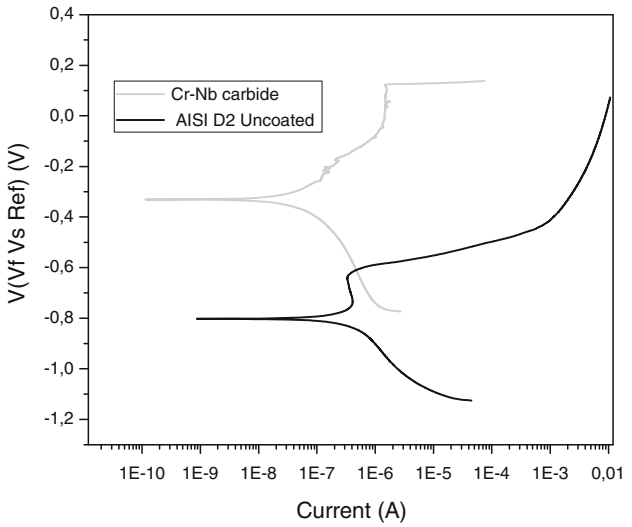

Fig. 9 Potentiodynamic curves for the AISI D2 steel uncoated and coated with the Nb–Cr complex carbide coating

In the Table 2 are shown the results obtained for the potentiodynamic polarization test using the Tafel extrapolation method. From the results of Fig. 9 and Table 2, it can be concluded that the Nb–Cr complex carbide-coated steel exhibited a greater corrosion resistance than the uncoated one. This conclusion can be drawn based on both the smaller current density (I_{corr}) and the higher value of the corrosion potential (E_{corr}) observed for the complex carbide when compared to the uncoated substrate. This performance can be explained by the chromium presence in the coating which is characterized by a good corrosion resistance.

Table 2 Results of the potentiodynamic polarization tests

System	I_{corr} (A)	E_{corr} (V)
(Nb–Cr) C	$9.0 \times 10^{-8} \pm 0.8 \times 10^{-8}$	-0.33666 ± 0.00047
AISI D2	$7.0 \times 10^{-6} \pm 0.9 \times 10^{-6}$	-0.80400 ± 0.00264

Despite their ceramic nature, the synthesized coatings exhibited corrosion potentials with negative values. This result is possibly due to the presence of porosity and other coherence defects in the coatings that allows the diffusion of the electrolyte to the coating–substrate interface, which could have enabled localized corrosion. In addition, the presence of galvanic couples originated at the grain boundaries of the coating could have accelerated the corrosion process. However, the electrochemical protection produced by the Nb–Cr carbide coatings was confirmed.

4 Conclusions

Nb–Cr complex carbide coatings were produced by TRD process onto AISI D2 steel using different processing times and temperatures.

The produced carbide layers exhibited a uniform thickness with values from 4.71 ± 0.23 to 15.30 ± 0.36 μm, depending on treatment time and temperature. The practical equations derived from classical kinetics expressions are very precise in the prediction of the layer thickness.

The EDS analyses showed the presence of Cr in the synthesized coatings and the XRD analysis showed the existence of an FCC phase, composed primarily of niobium carbide with a mixed orientation, mainly along the (200) and (311) planes, with small amounts of chromium carbide.

The coatings exhibited high hardness of 27.62 GPa, which is greater than the values reported for coatings of either CrC or NbC. This result is possibly due to substitution of Nb atoms by Cr atoms in the NbC crystalline structure.

The corrosion resistance of the AISI D2 steel coated with Nb–Cr complex carbide coatings was superior to that of the uncoated steel. However, the coatings did not exhibit the expected ceramic corrosion resistance, probably due to the presence of coherence defects, which allowed the electrolyte to penetrate to the substrate–coating interface, causing localized corrosion.

Acknowledgments The present work was supported by COLCIENCIAS project No. 338 of 2011. We are also very grateful to the Universidad Nacional de Colombia and to CSM Instruments.

References

1. Arai T, Fujita H, Sugimoto Y, Ohta Y (1987) Diffusion carbide coatings formed in molten borax systems. J Mater Eng 9(2): 183–189
2. Arai T, Harper S (1991) Thermo-reactive Deposition/Diffusion Process. In: ASM handbook, Heat treatment, vol 4. ASM International, Materials Park, pp 448–533
3. Oliveira CKN, Benassi CL, Casteletti LC (2006) Evaluation of hard coatings obtained on AISI D2 steel by thermo-reactive deposition treatment. Surf Coat Technol 201(3–4):1880–1885
4. Oliveira CKN, Muñoz-Riofano RM, Casteletti LC (2006) Microabrasive wear test of niobium carbide layers produced on AISI H13 and M2 steels. Surf Coat Technol 200(16–17):5140–5144
5. Sen S, Sen U, Bindal C (2005) The growth kinetics of borides formed on boronized AISI 4140 steel. Vacuum 77(2):195–202
6. Sen S (2005) A study on kinetics of CrxC-coated high-chromium steel by thermo-reactive diffusion technique. Vacuum 79(1–2): 63–70
7. Sen U (2004) Kinetics of niobium carbide coating produced on AISI 1040 steel by thermo-reactive deposition technique. Mater Chem Phys 86(1):189–194
8. Sinha AK 1991, Boriding (Boronizing). In: ASM handbook, Heat treatment, vol 4. ASM International, Materials Park, pp 437–447
9. Su YL, Kao WH (1998) Optimum multilayer TiN-TiCN coatings for wear resistance and actual application. Wear 223(1–2): 119–130
10. Worrell WL, Chipman J (1964) The free energies of formation of the vanadium, niobium, and tantalum carbides. J Phys Chem 68:860–866